Hindawi
Geofluids
Volume 2018, Article ID 7391517, 14 pages
https://doi.org/10.1155/2018/7391517

Research Article

The Monitoring-Based Analysis on Deformation-Controlling Factors and Slope Stability of Reservoir Landslide: Hongyanzi Landslide in the Southwest of China

Bing Han,[1] **Bin Tong**,[1] **Jinkai Yan**,[1] **Chunrong Yin**,[1] **Liang Chen**,[1] **and Deying Li**[2]

[1]*China Institute of Geo-Environmental Monitoring, Beijing, China*
[2]*Faculty of Engineering, China University of Geosciences, Wuhan, China*

Correspondence should be addressed to Bin Tong; tongb@mail.cigem.gov.cn

Received 28 February 2018; Accepted 8 May 2018; Published 10 July 2018

Academic Editor: Liangping Li

Reservoir landslide is a type of commonly seen geological hazards in reservoir area and could potentially cause significant risk to the routine operation of reservoir and hydropower station. It has been accepted that reservoir landslides are mainly induced by periodic variations of reservoir water level during the impoundment and drawdown process. In this study, to better understand the deformation characters and controlling factors of the reservoir landslide, a multiparameter-based monitoring program was conducted on a reservoir landslide—the Hongyanzi landslide located in Pubugou reservoir area in the southwest of China. The results indicated that significant deformation occurred to the landslide during the drawdown period; otherwise, the landslide remained stable. The major reason of reservoir landslide deformation is the generation of seepage water pressure caused by the rapidly growing water level difference inside and outside of the slope. The influences of precipitation and earthquake on the slope deformation of the Hongyanzi landslide were insignificant.

1. Introduction

Landslide induced by reservoir impoundment and drawdown is a commonly seen geological hazard in reservoir area and has caused significant impacts and damages on the operation and function of hydropower stations all over the world. Historical statistics show that in general, over 90% of reservoir-induced landslides are caused by the fluctuations of reservoir water level, and approximately 50% occurred during the period of impoundment [1–4]. More than 80% occurred during the first 3 to 5 years after the construction of the dam [1]. Regarding the influences of reservoir water level fluctuation, 40% occurred with the declination of reservoir water level [2, 3]. The large landslides of the sizes greater than ten million cubic meters were normally triggered by the rapid declination of the reservoir water level. Also, approximately 75% of triggered landslides were due to the revivification of ancient landslides [5]. In summary, the significant and instant reservoir water level fluctuations normally cause negative influences on the global stability of the reservoir slopes through influencing their hydrological conditions and reducing the slope strength [6].

The failure mechanisms and resulted chain of disasters (such as the impulse of wave) by reservoir landslides have been extensively studied in previous studies [5–7]. Erosions of loose debris at the slope toe by flow, instant pore water pressure generation in the slope by the drawdown of reservoir water level, and structural and strength reduction of the hydrofluctuation belt are the main reasons of triggering reservoir landslides [1, 4–6]. By conducting numerical analysis [6, 7], the risk management of potential impulse wave by the slope movement also draws more attentions. The majority of these researchers are intent to provide a complete overview/analysis on the whole process of the disaster chain, including the deformation triggering of the landslide to the

generation of impulse wave, as well as the resulted potential hazard to the properties in the reservoir or on the opposite bank [2, 3]. The full-process analysis offers valuable insights into the planning of prevention, control of geological hazards, and guidance on estimation of landslide-generated impulse waves in reservoirs.

Studies [7, 8] on reservoir landslide deformation characters indicated that the global deformation always started at the front part of the slope and mainly composed of the deformation of the slip band. The potential negative influences caused by the reservoir-induced landslides mainly include two aspects: (1) the significant reduction of reservoir storage capacity and water conservancy facilities operation due to the entrance of sliding material into reservoirs; (2) the formation of impulsive waves induced by sliding materials reaching the reservoir water with large dynamic energy and cause significant safety issues on the dam and the operation of hydropower stations [7, 9, 10].

The slope monitoring technology developed rapidly over the past several decades. At the beginning of 21th century, the optical fiber monitoring system became more extensively used, and advancements of higher accuracy, greater speed, and higher automation in monitoring technology have occurred. Meanwhile, one of the important problems to be solved is to improve the coordination and integration of the monitoring system of involving different types of monitoring devices for various monitoring parameters. Currently, the data communication and compatibility of the data processing software for comprehensive slope dynamic performance is a major research issue.

Therefore, it is important in theory and engineering practice to study the impact and casual correlations among reservoir water level fluctuation, hydrodynamic, and deformation characters of reservoir landsides. Conducting the comprehensive monitoring program on reservoir landslides is the key issue of obtaining the in situ data, which set the basis for conducting the more comprehensive analysis and simulations. The periodic geological inspections are recommended to monitor the deformation and hydrogeological condition of the slope during the process of reservoir water level fluctuation [4, 11].

In this paper, a multiparameter monitoring program was conducted to record the change of ground water level, surface deformation, and deep-seated displacement at various locations on the Hongyanzi landslide, located in Pubugou Hydropower Station reservoir area, Sichuan province, Southwest China, during the period of reservoir impoundment and drawdown from 2013 to 2014.

Based on the measurements, the temporal correlations among reservoir water level fluctuation, slope groundwater level, surface displacements, crack propagations, and deep-seated displacement are interpreted. The preliminary recommendations are made to help control the negative influences of reservoir water level fluctuation on the slope stability of reservoir landslides. The findings presented in this paper could also offer the valuable insights into the planning of prevention and control of geological hazards in the Pubugou Hydropower Station reservoir area and relevant studies on reservoir induced landslides in the world.

Figure 1: Location map of the Hongyanzi landslide (source: Google Earth).

Figure 2: 3D view of the Hongyanzi landslide.

2. Overview of the Hongyanzi Landslide

The Hongyanzi landslide is located in the right bank of the Dadu River, a secondary tributary of the Yangtze River in Hanyuan County, Sichuan province in the Southwest of China (Figure 1). It is 23 km away from the Pubugou Hydropower Station in the downstream region. According to the previous investigations, the overall slope of the Hongyanzi landslide is 27 degrees. The slope magnitude varies significantly along the surface the landslide from the scarp to the toe.

The plan view of the Hongyanzi landslide is approximately semicircular (Figure 2). The sliding direction is 340 degrees. The elevation of the slope toe and back-scarp is 810 m and 954 m, respectively, and the overall elevation difference between the toe and the slope is approximately 150 m. The total length and width are 600 and 580 m, respectively [10].

Prior to the installations of monitoring devices, the large deformations have occurred to both left and right boundaries, and the magnitude reached 1.7 m and 1.5 m, respectively, due to the reservoir water fluctuation during the same period. According to the in situ investigation [10], the thickness of sliding material is nonuniform, and the thickness varies from 20 to 50 m over the entire slope area. Since the Hongyanzi landslide is an ancient landslide, the thickness of sliding material in the front is greater than that in the rear. Geomorphologically, the plain area of Hongyanzi landslide is

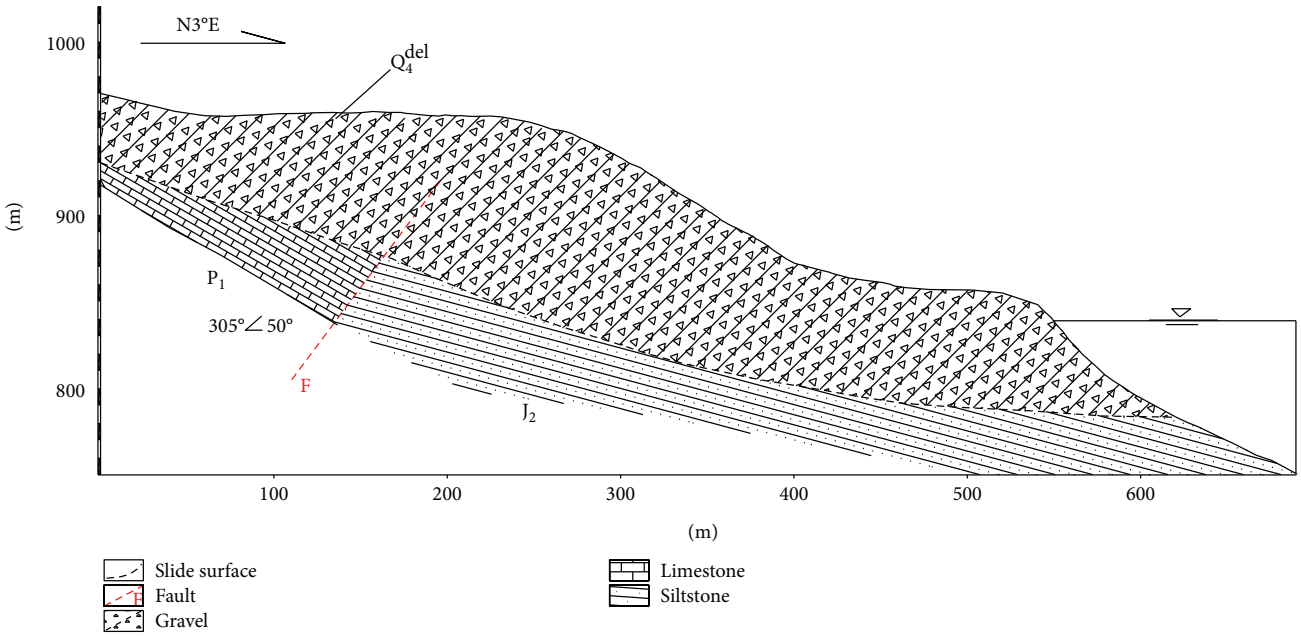

Figure 3: Main geological profile of the Hongyanzi landslide.

about $1.80 \times 10^5\,m^2$, and the total volume is approximately 7.7 million m^3. The sliding surface is flatter in the front and steeper in the rear, and slope difference is about 20 degrees [10]. Due to the large distortions occurred to the pavements on the slope, the boundary of the Hongyanzi landslide can be easily identified in the field.

Based on field investigation, the Hongyanzi landslide is an ancient accumulation landslide (Figure 3), and the sliding material is mainly composed of the quaternary silty clay, cobble, or gravel, and the stones of diameter from 1 to 3 meters can be observed locally. The primary composition of cobble and gravel is limestone with a densely compact structure. The stratum of sliding bed is Jurassic reddish sandstone in the footwall of Hanyuan-Zhaojue fault and Permian limestone in hanging wall of the fault [10].

The hydrogeological condition of the Hongyanzi landslide is relatively simple. The groundwater is mainly the pore phreatic water in loose rock mass, and the major supply is atmospheric precipitation. The Hongyanzi landslide faces the Dadu River in the north and gullies in the east and west. The steep topography and large elevation differences from the scarp to the toe provide a great potential for groundwater to discharge into the Dadu River. During the operation of the Pubugou Hydropower Station, the reservoir water level varied from 790 m to 850 m, and the range of water-level-fluctuating zone was approximately 60 m. The fluctuation of reservoir water level had a vital impact on the ground water table of the reservoir bank slopes.

Based on the historical records [10], the Hongyanzi landslide remained stable before the construction of the hydropower station. After the impoundment, large deformation occurred to the Hongyanzi landslide during the declination period of the reservoir water level. The impoundment and power generation started on June and November 2010, respectively. In February 2011, after 8 months of impoundment, large deformations occurred to the Hongyanzi landslide and the accumulated downward deformation reached up to 1 m by the end of 2011 depending on the local topography. Simultaneous deformation continued to occur with the declination of reservoir water level in 2012. From 2013 to 2014, the maximum deformation reached to 2.7 meters, and the accumulated deformation since the beginning of hydropower station operation is more than 4 meters. The majority of the deformations occurred during the declination of the reservoir water level, and no large deformations were observed when the reservoir water level remains stable or increases. Similar observations were also made by previous studies [12–18]. Due to the extensive deformation of the Hongyanzi landslide, a multiparameter monitoring program was conducted on the Hongyanzi landslide to advance the understanding on the deformation characters and its major influencing factors.

3. The Multiparameter Monitoring

Since 2012, various monitoring equipment (Figure 4 and Table 1) were employed to conduct a continuous monitoring program on the simultaneous developments of surface deformation, deep-seated deformation, ground water table in the slope, crack propagations on the left and right boundaries, and the atmospheric precipitations. Reservoir level was measured by the water gauge. The distribution of the installed monitoring devices is shown in Figure 4. The monitoring program started in January 2013, and this study mainly focuses on the monitoring data received prior to December 2014.

3.1. Slope Ground Water Table. As shown in Figure 5, a strong correlation exists between slope water level in ZK-5-w and reservoir water level. The reservoir water level declined

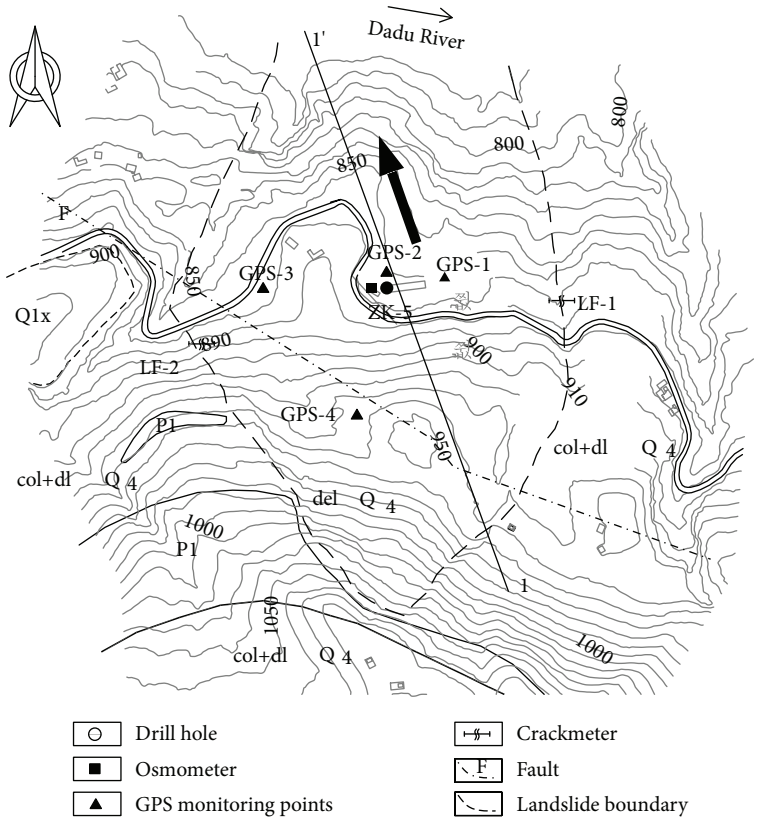

Figure 4: Distribution of monitoring devices on Hongyanzi landslide.

Table 1: Monitoring devices employed in this study.

Device ID	Measuring data and installed location
GPS-1	Surface displacement (on the right of the center)
GPS-2	Surface displacement (middle part of landslide)
GPS-3	Surface displacement (on the left of the center)
GPS-4	Surface displacement (near the scarp)
LF-1	Surface crack propagation (on the right boundary)
LF-2	Surface crack propagation (on the left boundary)
ZK-5-d	Deep-seated displacement (middle part of landslide)
ZK-5-w	Ground water table (middle part of landslide)

gradually from January to April 2013 from 850 m to 792 m. Meanwhile, the slope water level measured in ZK-5-w also decreased from 853 m to 825 m. In May, the reservoir water level started rising and reached 842 m in July. At the same time, the slope water level returned to 846 m. In August, the reservoir water level decreased from 842 m to 819 m, and the slope water level also decreased from 847 m to 834 accordingly. During the initial of the drawdown period, the declination rate of the slope water level is roughly the same with the value of reservoir water level. However, when the reservoir water level declined with increased speed, the declination of slope water level lags behind.

3.2. Surface Displacement. Four GPS monitoring stations were installed on the slope surface, and the measuring results showed that large slope deformations, which mainly

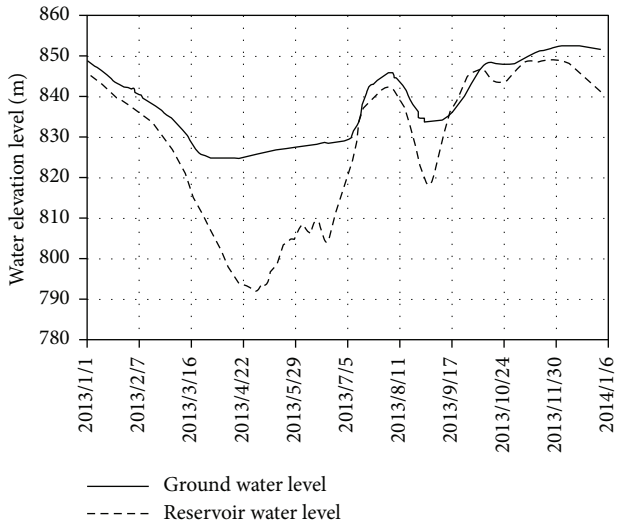

Figure 5: Reservoir water level versus ground water level.

occurred to from March to June, were captured from 2013 to 2014. The directions of the horizontal displacements measured by GPS-1, GPS-2, and GPS-3 that were located in the mid to front of the slope were approximately the same (NW 22 to 24 degrees). The magnitude of displacements also increased from left to the right on the slope. The maximum horizontal and vertical displacement was 2690 mm (GPS-1) and 760 mm (GPS-3), respectively. GPS-4 was located near a steep scarp in the midrear part of the slope. Therefore,

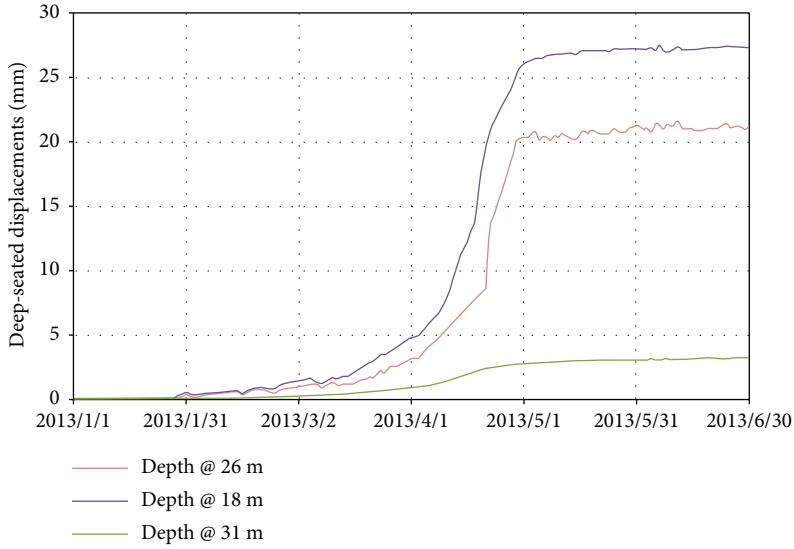

Figure 6: Reservoir water level versus deep-seated resultant displacement (ZK-7-d).

due to the influence of microtopography on the measurements, the deformation characters captured by GPS-4 were different from the other three stations. The direction of horizontal displacement at GPS-4 was NW 16 degrees, and the horizontal and vertical displacements were measured to be 1780 mm and 2000 mm, respectively.

Crack propagations were also monitored on the east and west boundaries of the Hongyanzi landslide. From January to July 2013, especially from April to July 2013, the crack development (LF-1) on the east boundary was significant, and the magnitude reached 1400 mm. On the contrast, crack propagated (LF-2) much lower on the west boundary, and the magnitude reached only 180 mm. Above measurements received good agreements with the surface displacements measured by GPS receivers, which clearly showed that the surface compression and tension occurred on the west and east boundaries, respectively. Also, the recording on both boundaries showed a consistent temporal correlation with surface displacement recorded by GPS stations.

3.3. Deep-Seated Displacement. The measuring depths for deep-seated displacement at ZK-7-d are 18 m, 26 m, and 31 m. Figure 6 shows that small magnitude of deformation of less than 5 mm occurred at a depth of 31 m, and the deformations at the depths of 18 m and 26 m were much larger. This could provide a good support for determining the elevation of sliding surface and volume of sliding material. Similar to the surface displacement and ground water table, a clear and consistent temporal correlation exists between the deep-seated displacement and fluctuation of reservoir water level as shown in Figure 7. Similar to the occurrence time of surficial deformation, the large deep-seated displacement started to increase in ZK-7-d from March to May.

3.4. Precipitation. According to the precipitation record at the Hongyanzi landslide, the average annual precipitation is approximately 400 mm and mainly concentrates from May to August, as shown in Figure 8. Based on the correlations among the 1-day precipitation (Figure 9), 3-day accumulative precipitation (Figure 10), and slope deformation, it was found that significant deformation occurred during the period from March to April while no intensive precipitation was observed. In June, however, no large deformation was captured while intensive precipitation was recorded. Therefore, based on the above observations, the influence of rainfall on the development of landslide deformation could be fairly insignificant. Additional monitoring is being conducted currently to further analyze the influence of precipitation on the Hongyanzi landslide deformation.

3.5. Influence of Earthquake Events on Deformation of Hongyanzi Landslide. On April 20, 2013, an earthquake event of magnitude 7.0 hit the Lushan country, Sichuan province, and the distance from Hongyanzi landslide to the epicenter is about 100 km and the magnitude of intensity is VI. The recorded peak acceleration by the seismic station closest to Hongyanzi landslide was 0.4g. A postearthquake field investigation was conducted, and the deformations on the boundaries were found larger than the routine deformation magnitudes induced by reservoir water fluctuations. The surface distortions of 50 mm and 10 mm were observed on the right and left boundaries, respectively. No obvious increases in the surface and deep-seated displacements were recorded by the monitoring devices.

4. Influence of Reservoir Water Level Fluctuation on Slope Stability

As shown in Figure 11, the primary deformations occurred during the drawdown period from March to April, especially when the declination rate was large. Other than that, no deformation was recorded during the impoundment period. Among the GPS measuring stations, the maximum deformation recorded by GPS-1 was the greatest and the magnitude reached 1823 mm in 2013, of which 1526 mm occurred from March to April. Meanwhile, the reservoir water level declined

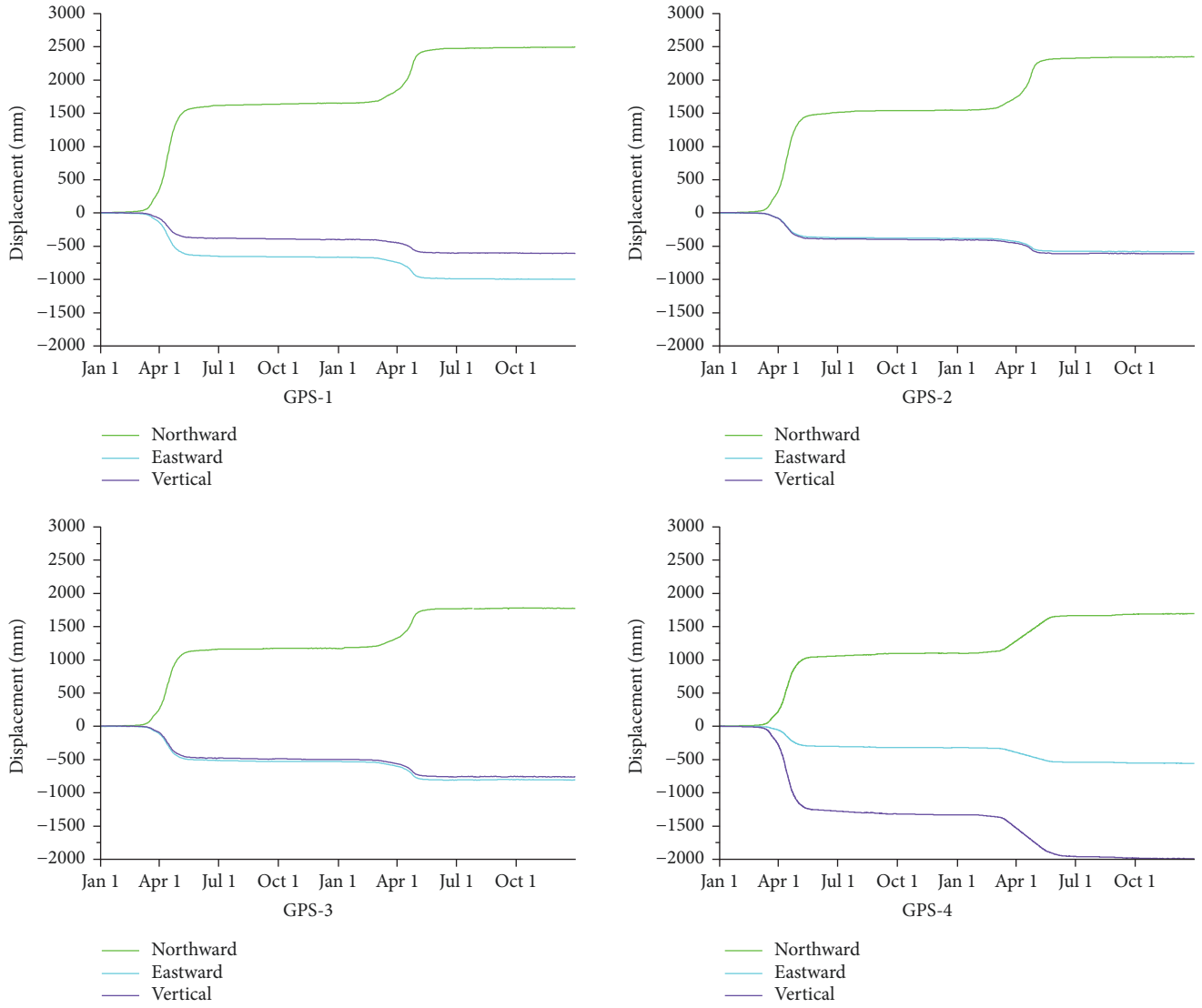

Figure 7: Surface displacement measurements at various GPS stations.

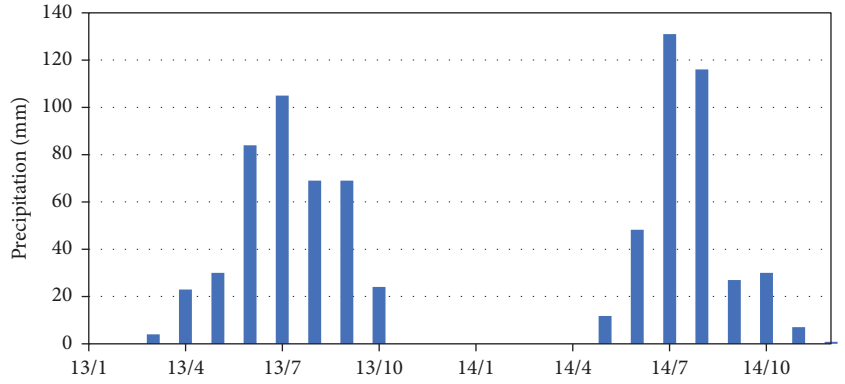

Figure 8: The monthly average precipitation amount from Jan. to Oct. in 2013 and 2014.

to 35.9 m. The overall deformation occurred in 2014 was approximately 932 mm, of which 730 mm occurred from March to April. Meanwhile, the reservoir water level declined to 30.6 m. The similar correlation between reservoir water level and slope deformations was captured by the other GPS stations.

Based on the correlation between the magnitude of daily drawdown of reservoir water level and the slope deformation

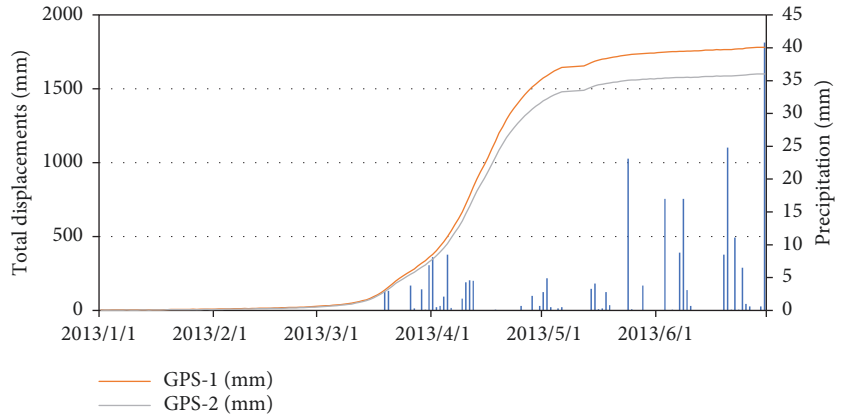

Figure 9: Total displacements measured by GPS versus daily precipitation.

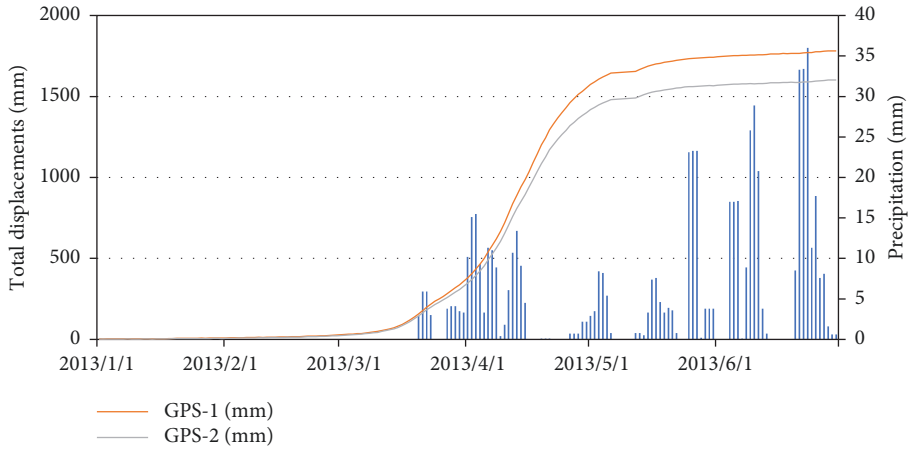

Figure 10: Total displacements measured by GPS versus precipitation in accumulative 3 days.

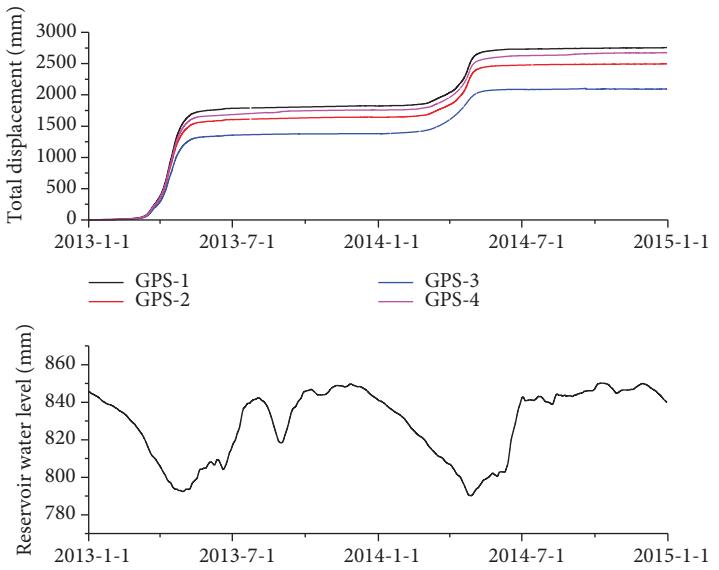

Figure 11: Surface displacements by GPS measuring stations versus reservoir water level fluctuations.

captured by GPS station (Figures 12 and 13), the deformation was insignificant from January to February when the drawdown rate was less than 0.5 m/day. From March to April, the drawdown rate increased rapidly, and the magnitude exceeded 0.5 m/d. Meanwhile, significant slope deformations were captured by all GPS measuring positions, and the

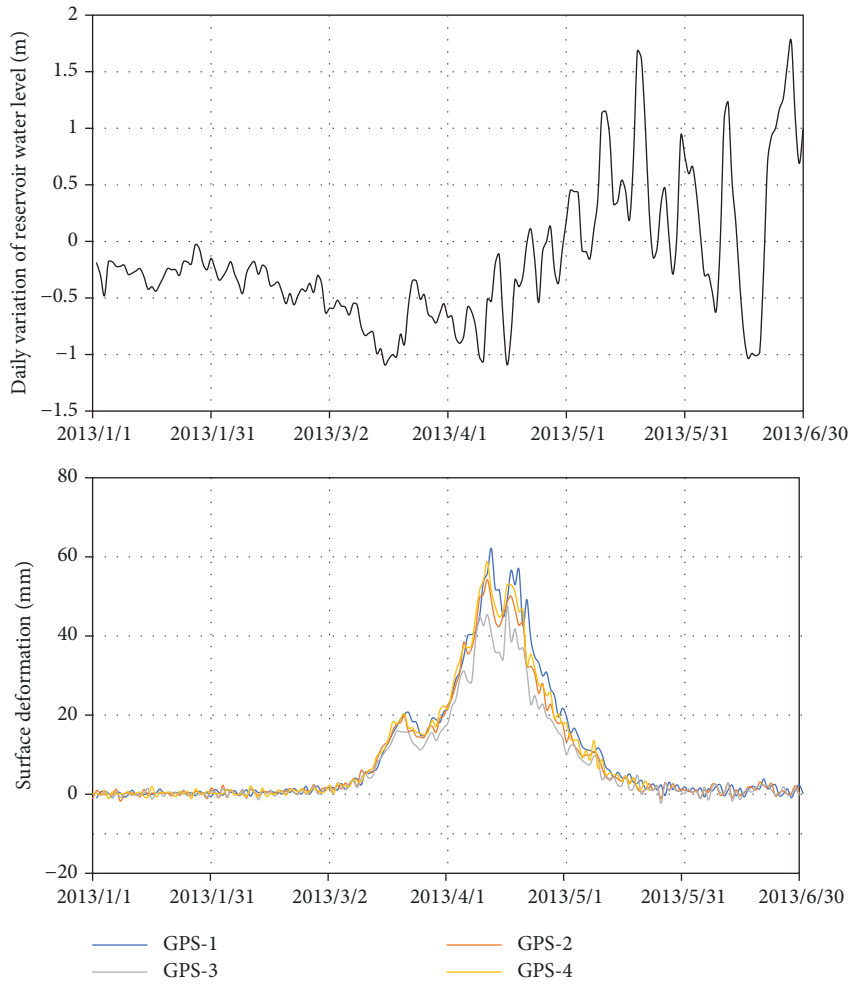

Figure 12: The magnitude of daily drawdown of reservoir water level from January to June 2013 versus surface deformation measured by GPS.

deformation rate showed an acceleration trend in an overall stable condition. From March 22 to 24 and April 13 to 14, the drawdown rate magnitude of reservoir water level decreased slightly, and also the deformation rate at all GPS measuring positions showed the declined trend.

From May, the reservoir water level started to rise, and daily rate of deformation deceased rapidly accordingly. After June, the deformation measurements at all GPS stations became stable gradually. Therefore, the deformation of the Hongyanzi landslide is related to the drawdown rate of Pubugou reservoir water level, and the magnitude of 0.5 m/day can be regarded as critical value based on the correlation between the slope deformation and drawdown magnitude.

A groundwater gauge was installed at ZK-5 to capture the correlation between the magnitude of water level difference (slope ground water minus reservoir water level) and deformation measurements. As seen from the correlation in Figure 14, before February 2013, the water level difference remains stable with slight increases, and similarly, during the same period, the slope deformation was also insignificant; from the beginning of February to the mid of March, with the increase of water level difference inside and outside the slope, the slope deformations measured at all GPS positions increased; after the mid of March, significant increase occurred to all the measurements when the water level difference was approximately 10 m. Therefore, the increased water level difference between slope ground water level and reservoir water level has significant influence on the slope deformation.

The recordings indicated deformation mechanism that the rapid declination of reservoir water level increased the hydraulic gradient of groundwater and seepage in the slope, which further change the pore water pressure, decrease effective strength, and reduce the slope stability by decreasing the buoyant force acting on the slope.

To further quantify the influence of controlling factors on slope deformation, the SPSS software was utilized to conduct the correlation analysis among slope groundwater level, surface displacement (measured at GPS-2), reservoir water level, and precipitation. The results indicated that the difference between slope groundwater level and reservoir

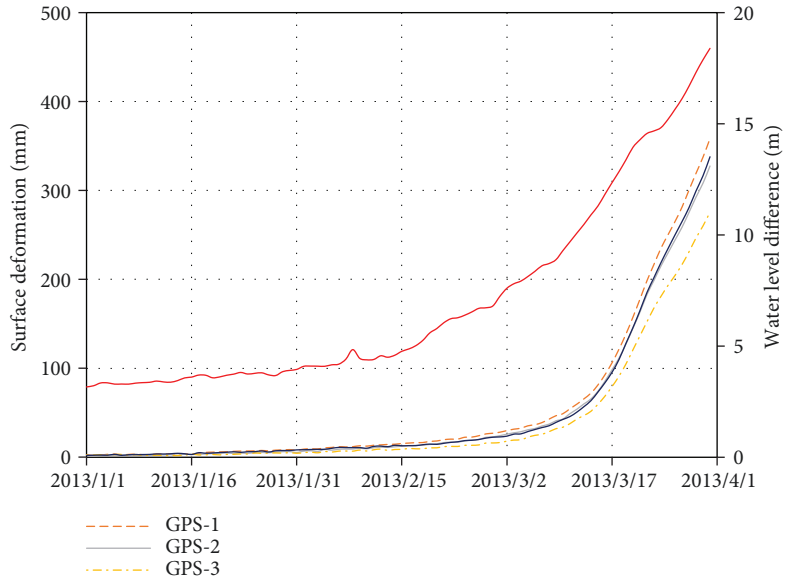

Figure 13: Water level difference inside and outside the slope versus surface measurements by GPS.

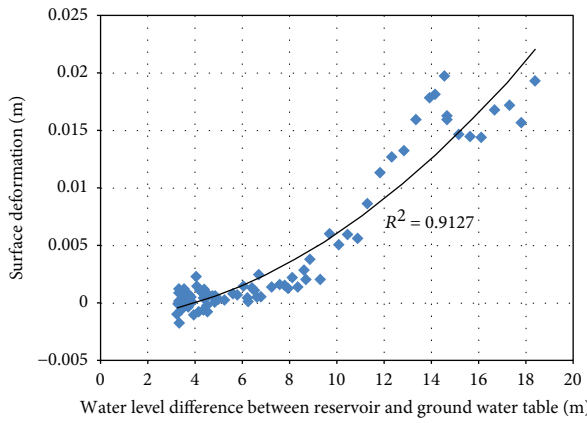

Figure 14: Correlation between the water level difference inside and outside the slope versus daily slope deformation in ZK-5.

water level showed the most statistical importance to the slope surface displacement (correlation coefficient = 0.926) and followed by reservoir water table (coefficient = 0.785). The correlation between precipitation and slope surface displacement is the lowest.

Based on the correlation between slope daily deformation and water level difference, a good consistency between can be observed. When the water head level difference was less than 7 m, the slope remained approximately stable and the deformation magnitude was insignificant. When the water level difference exceeded 7 m, the slope deformation also increased with the increases of water level difference, and the result can be fitted with quadratic function with determination of coefficient of 0.91.

Based on the above analysis, the major triggering mechanism of deformation is the rapid drawdown of reservoir water level, which caused the insufficient drainage of the water in the slope and increased water level difference inside and outside the slope. The increased water level difference inside and outside the slope also leads the increase of seepage force. Then the seepage force reaches the threshold value; the slope deformation would be triggered.

4.1. Slope Model Establishment. Based on the field survey data, the two dimensional model of the Hongyanzi landslide was produced and the dimensions of the model is 670×210 m (in Figure 15). The base of the model was set as impermeable, and the left boundary was set to the fixed water head level of 850 m. When calculating the slope stability during the drawdown period, the right boundary above the reservoir water level is set as the zero flux. Below the reservoir water level, it was set as flexible flux boundary, and the water head equalled to the reservoir water level. When calculating the slope stability during the rise of the reservoir water level, the right boundary above 845 m is set as zero flux, and below 845 m was set as flexible flux, which the water head level equalled to the reservoir water level. The surface of the slope was set as the boundary of fixed flow, and the magnitude was set to be the amount of precipitation. The entire model consists of 1031 nodes and 990 meshes.

4.2. Parameters. According to the field investigation results, the major parameters used in simulation are presented in Table 2. The parameters being used in the numerical simulation is based on the experimental results conducted on the soil samples obtained in the field and the average value for each parameter was employed to eliminate the potential errors.

The slope ground water in natural condition is above the slip surface, and the saturated hydraulic coefficient is assumed to be 0.45 m/day; the characteristic curve between soil and water and permeability function for the upper part

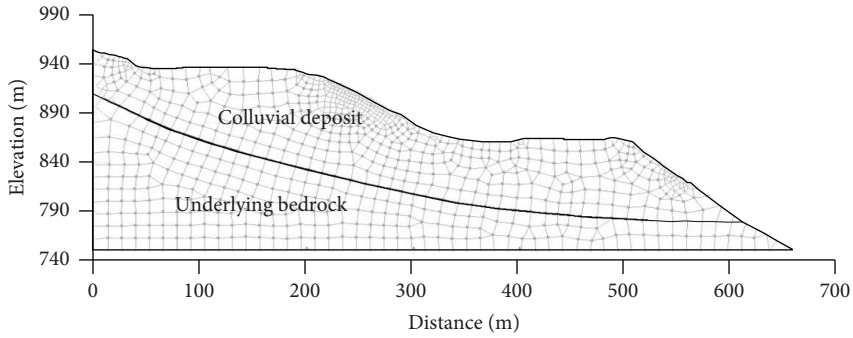

Figure 15: The established model of Hongyanzi landslide (unit: m).

Table 2: Physical parameters used in numerical simulation.

Zone	Saturated hydraulic coefficient (m/d)	Effective cohesive force (kPa)	Internal friction force (degree)	Dry density (g/cm^3)	Saturated density (g/cm^3)
Debris flow deposit	0.45	22	12.9	2.3	2.7
Underlying bedrock	0.001	3200	44	2.6	3.0

of the slope (unsaturated) was generated using the module in Seep/W, which was based on Fredlund-Xing theory.

4.3. Mathematical Model for Seepage Calculation of the Unsaturated Condition. The slope seepage analysis is one of the main issues in this study. Considering the homogeneous formation and uniform conductivity properties in various direction of the Hongyanzi landslide, the plane seepage theory based on saturated and unsaturated soils could be considered in this analysis.

Based on Morgenstern and Fredlund's theory, the nonsteady seepage condition always involves the variation of flow rate, water level pressure head, and quality of flux with time. Therefore, the following equation could be produced based on two stress variables to calculate the volume water content θ_w, and the two stress variables are normal stress $(\sigma - u_a)$ and matric suction $(u_a - u_w)$.

$$d\theta_w = -P_1^w d(\sigma - u_a) - P_2^w d(u_a - u_w). \quad (1)$$

In the equation, σ is the total pressure; u_a and u_w is the pore air pressure and pore water pressure, respectively; P_1^w and P_2^w are the correlation coefficients related to $(\sigma - u_a)$ and $(u_a - u_w)$ for the water volume.

Within the infinite short time period, the P_1^w and P_2^w can be regarded as constants in the calculation; therefore, (2) can be rewritten as follows:

$$\frac{\partial}{\partial t}\theta_w = -P_1^w \frac{\partial}{\partial t}(\sigma - u_a) - P_2^w \frac{\partial}{\partial t}(u_a - u_w). \quad (2)$$

Then, the mathematical expression for the nonsteady seepage condition is

$$\frac{\partial}{\partial x}\left(k_x \frac{\partial h}{\partial x}\right) + \frac{\partial}{\partial z}\left(k_z \frac{\partial h}{\partial z}\right) = -P_1^w \frac{\partial}{\partial t}(\sigma - u_a) - P_2^w \frac{\partial}{\partial t}(u_a - u_w). \quad (3)$$

Considering that the pore air pressure is continuous and constant within the infinite short time period, and no external load was applied during the seepage condition, then,

$$\frac{\partial \sigma}{\partial t} = 0, \quad \frac{\partial u_a}{\partial t} = 0. \quad (4)$$

Therefore,

$$\frac{\partial}{\partial x}\left(k_x \frac{\partial h}{\partial x}\right) + \frac{\partial}{\partial z}\left(k_z \frac{\partial h}{\partial z}\right) = -P_2^w \frac{\partial}{\partial t}(u_a - u_w), \quad (5)$$

where $P_2^w(\partial/\partial t)(u_a - u_w)$ is the slope magnitude of the soil-water characteristic curve.

Considering the total pressure head can be expressed as follows:

$$h = y + \frac{u_w}{\gamma_w}, \quad \frac{\partial y}{\partial t} = 0, \quad \frac{\partial u_a}{\partial t} = 0. \quad (6)$$

Therefore, the total pressure head can be expressed using u_w as follows:

$$\frac{\partial}{\partial x}\left(k_x \frac{\partial h}{\partial x}\right) + \frac{\partial}{\partial z}\left(k_z \frac{\partial h}{\partial z}\right) = \rho_w g P_2^w \frac{\partial h}{\partial t}. \quad (7)$$

In conclusion, the definite conditions of the unsaturated seepage condition can be expressed using the above mathematical equations. Based on the theoretical derivations, the correlations between the water content and matric suctions and the hydraulic conductivity and matric suctions of the Hongyanzi landslide can be plotted using the calculation module in Seep/W, and the results are presented in

Figures 16 and 17, respectively. The curves show the general characters of the soil-water characteristic and nonsaturated permeability of the analyzed landslide.

$$h(x, y, t) = H_1(x, y, t), \text{ the boundary of the pressure head is known,}$$
$$K_x \frac{\partial h}{\partial x} \cos\left(\vec{n}, x\right) + K_z \frac{\partial h}{\partial z} \cos\left(\vec{n}, z\right) = q,$$
$$h(x, y, t) = y(x, y, t),$$
$$h(x, y, t_0) = H_0(x, y, t_0). \tag{8}$$

4.4. Slope Stability Analysis. In this study, the slope/w module was applied to calculate the slope stability based on Morgenstern-Price limit equilibrium state theory. Morgenstern-Price theory is regarded as the most comprehensive limit equilibrium state theory by considering the mechanical and moment equilibrium currently [12, 14]. The method assumes the functional relationship between the tangential and normal stress among the soil slices. The mathematical expression of the factor of safety calculation is as follows:

$$F_s = \frac{\sum\left(c' l_i + \left[N - u_w l_i \left(\tan \varphi_b / \tan \varphi'\right) - u_a l_i \left(1 - \tan \varphi_b / \tan \varphi'\right)\right] \tan \varphi'\right)}{\sum W_i \sin \theta_i}, \tag{9}$$

where τ_f is the shear strength of unsaturated soil; c' is the effective cohesive force of the saturated soil; φ' is the effective friction angle; φ^b friction angle based on the matric suction. The value of φ^b can be regarded as regional value φ and constant for saturated and nonsaturated conditions, respectively.

And, the parameter N in above equation can be expressed as follows:

$$N = \frac{W - (X_R - X_L) - \left(\left(c' l_i \sin \theta_i / F_s\right) + \left(u_w l_i \sin \theta_i \tan \varnothing^b / F_s\right)\right)}{P_{\theta i}}, \quad P_{\theta i} = \cos \theta_i + \frac{\sin \theta_i \tan \varnothing'_i}{F_s}. \tag{10}$$

where W is the weight of soil slice; X_L and X_R are the shear stress applied on the soil slices on the left and right boundaries, respectively; r is the radius of slicing surface; S_{mi} is the antisliding force on the base on the soil slice; θ_i is the angle between the tangent line of the soil slice base center and horizontal line.

A two-dimensional landslide stability analysis was conducted using the Geostudio software. The analytical module Seep/W was used to analyse the slope seepage condition changing with the fluctuations of reservoir water level and precipitation, and the slope ground water table, pore water pressure, and water head distribution of the seepage condition could be generated; then, apply the simulation results of seepage analysis into the slope stability analysis by the slice method using the module Slope/W, and the slope stability under different fluctuation rate of reservoir water level can be produced.

4.5. Numerical Simulation Verification. In this simulation, the monitoring data of the reservoir water level fluctuations and precipitation was used as input, and the results, as shown in Figure 18, indicated that the simulated slope ground water level of ZK-5 is approximately the same with the monitoring data, which provide good support for the set of the boundary conditions and parameters of the numerical simulation.

4.6. Landslide Slope Stability Analysis. Based on the simulation results, the Hongyanzi landslide remained stable under the condition without impounding, and the safety of factor is calculated to be 1.22 approximately (in Figure 19).

To understand the influence of reservoir water level fluctuations on slope stability, numerical simulation was conducted to calculate the slope stability when the fluctuation rate of reservoir water level equals from 0.1 to 0.7 m/day. The results show that during the impounding period, the slope ground water and pore pressure increased accordingly. A greater rising rate of reservoir water level could lead to the increased pore water pressure within a fixed time, which would further reduce the slope stability. When the rising rate equals to 0.7 m/d, the slope safety factor becomes 1.1 and the slope remains stable. During the drawdown period, when the drawdown rate of reservoir water level gradually increased, the slope ground water may not be dissipated sufficiently, which would lead to an increased water level difference and reduced slope stability. At the drawdown rate of 0.7 m/d, the minimum safety factor of the slope is 0.995 based on calculation results (Table 3).

As shown in Figure 20, when the drawdown rate of the reservoir water level equals to 0.1 and 0.3 m/d, the safety factor of the Hongyanzi landslide increased gradually after a slightly increasing trend. When the drawdown rate exceeded 0.4 m/d, the slope stability continued decreasing. The major

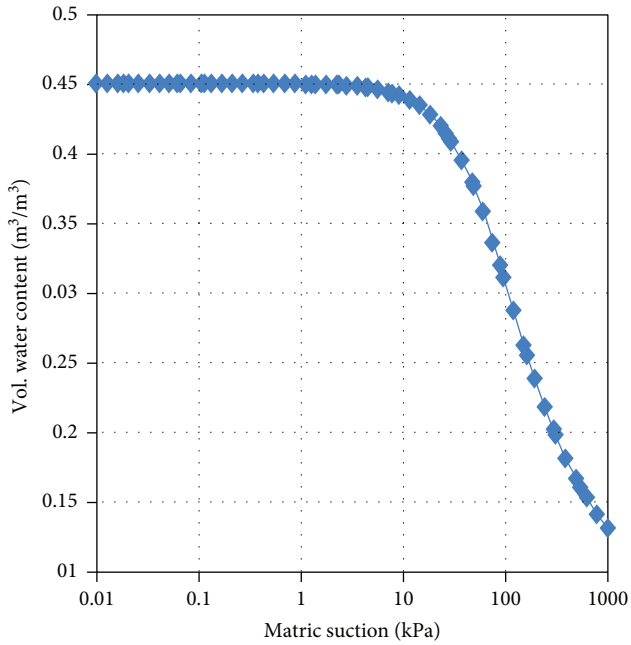

Figure 16: Soil-water characteristic curve of the Hongyanzi landslide.

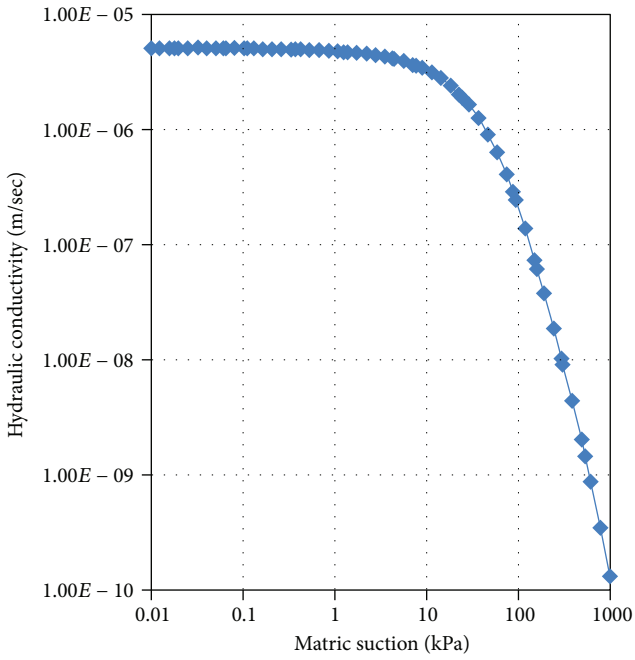

Figure 17: Nonsaturated permeability curve of the Hongyanzi landslide.

reason is that when the drawdown rate of the reservoir water level is fairly low, the stability was reduced due to the increased seepage force. On the other hand, the drawdown of reservoir water level caused the reduction of slope weight, which could increase the slope stability. When the drawdown rate is fairly large, the influences of seepage force play significant and negative impact on the slope stability.

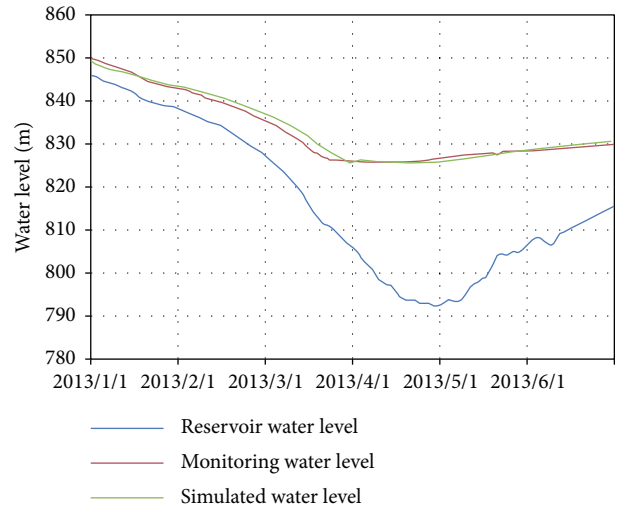

Figure 18: Comparison between simulated and monitored slope water level.

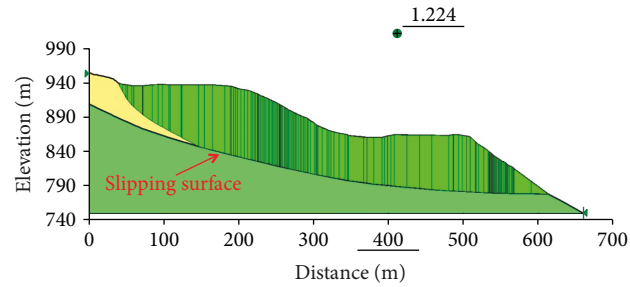

Figure 19: The stability calculation results without impounding of the reservoir water level (unit: m).

Table 3: The calculation results of FOS during the rise and decline of the reservoir water level.

Rate of fluctuation	0.1 m/d	0.3 m/d	0.4 m/d	0.5 m/d	0.7 m/d
Rising period	1.180	1.169	1.156	1.119	1.105
Decline period	1.119	1.091	1.077	1.013	0.0995

When the drawdown rate of reservoir water level equals to 0.1 to 0.4 m/d, the slope safety factor is greater than 1.05, and the slope remains stable; when the rate increased to be 0.5 m/d from 0.4 m/d, the slope safety factor reduced rapidly. The monitoring stations also indicated that when the drawdown rate of reservoir water exceeded 0.5 m/d, the slope deformation increased significantly.

The saturated hydraulic coefficient of Hongyanzi landslide is 0.45 m/d, between 0.4 m/d and 0.5 m/d. Based on the initial analysis, when the drawdown rate of reservoir water level is greater than the saturate hydraulic conductivity of the slope, the increase of water level difference and seepage pressure would lead to the reduction of slope stability. On the contrast, when the declination rate of reservoir water level is lower than the slope hydraulic conductivity, the influence of reservoir water level decline is fairly limited to the slope stability.

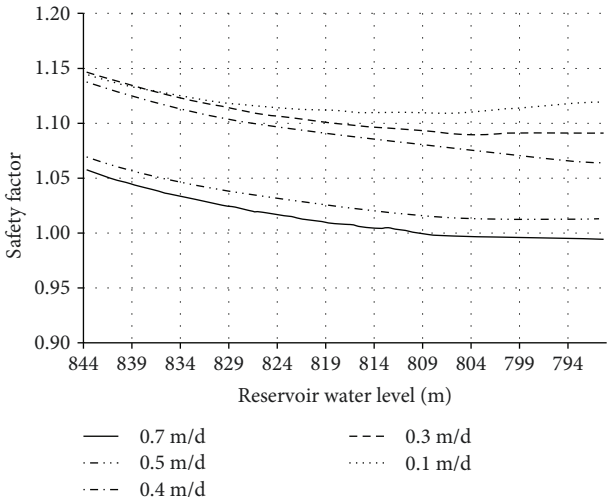

Figure 20: The variations of slope safety factor under different reservoir water level declination rate.

5. Conclusions

By conducting the multiparameter monitoring program on a reservoir landslide—the Hongyanzi landslide, the controlling factors of slope deformation were analysed and safety factor was calculated when the slope was hypothetically subjected to different rising rate of reservoir water level. The major conclusions are listed as below:

(1) The Hongyanzi landslide was more prone to deformation during the rapid reservoir water level declination period, and otherwise, the slope remained stable. The slope deformation was insignificant under the intensive rainfall and earthquake conditions (e.g., Lushan earthquake) based on the captured data as presented in this study. It is recommended to conduct further monitoring on the influence of intensive rainfall and earthquake loadings on the deformation of the Hongyanzi landslide for further analysis.

(2) The primary triggering mechanism of slope deformation is due to the increased seepage force generated by the increasing water level difference inside and outside the slope during the rapid declination of the reservoir water level. Roughly, there was a quadratic function relationship between the magnitude of slope water level difference and slope deformation.

(3) The declination rate of reservoir water level has a vital impact on slope stability. The increasing of declination rate would lead to the decreased slope stability. When the declination rate exceeded 0.7 m/day, the slope stability factor would become less than 1.

(4) The major characters of slope monitoring technology system are automation, wireless sensing, distributed arrangement, and high accuracy. It is anticipated that the multiparameter-based monitoring as used in this study can be helpful to improve the coordination and integration of slope monitoring system.

Data Availability

The authors welcome the other researchers to cite and analyse the data of this paper in their studies. If you need the data, please send an e-mail to hanb@mail.cigem.gov.cn.

Conflicts of Interest

The authors wish to confirm that there are no known conflicts of interest associated with this publication.

Acknowledgments

The research data of this study is mainly from the "Sichuan Ya'an Geological Hazard Monitoring and Warning Field Scientific Observation and Research Base of the Ministry of Land and Resources of China." The study was funded by China Geological Survey Projects (Grant nos. 1212011140016 and DD20160273), Chinese Key Science and Technology Project (Grant no. 2010ZX03006-007), and China Geological Environment Monitoring and Forecasting Project.

References

[1] H. Tang, C. Li, X. Hu et al., "Deformation response of the Huangtupo landslide to rainfall and the changing levels of the Three Gorges Reservoir," *Bulletin of Engineering Geology and the Environment*, vol. 74, no. 3, pp. 933–942, 2015.

[2] Y. Yin, B. Huang, W. Wang et al., "Reservoir-induced landslides and risk control in Three Gorges project on Yangtze River, China," *Journal of Rock Mechanics and Geotechnical Engineering*, vol. 8, no. 5, pp. 577–595, 2016.

[3] J. B. Wei and H. C. Zheng, "Deformation characteristics of a preexisting landslide in reservoir area during reservoir filling and operation," *Advanced Materials Research*, vol. 518–523, pp. 4675–4679, 2012.

[4] Y. Y. Jiao, H. Q. Zhang, H. M. Tang, X. L. Zhang, A. C. Adoko, and H. N. Tian, "Simulating the process of reservoir-impoundment-induced landslide using the extended DDA method," *Engineering Geology*, vol. 182, pp. 37–48, 2014.

[5] F. C. Dai, J. H. Deng, L. G. Tham, K. T. Law, and C. F. Lee, "A large landslide in Zigui County, Three Gorges area," *Canadian Geotechnical Journal*, vol. 41, no. 6, pp. 1233–1240, 2004.

[6] J. Jiang, D. Ehret, W. Xiang et al., "Numerical simulation of Qiaotou landslide deformation caused by drawdown of the Three Gorges Reservoir, China," *Environmental Earth Sciences*, vol. 62, no. 2, pp. 411–419, 2011.

[7] G. Y. Liu, "Influence of water table fluctuation on stability of colluvial landslide in Three Gorges Reservoir," *Safety and Environmental Engineering*, vol. 18, no. 5, pp. 26–28, 2011.

[8] B. Huang, Y. Yin, and C. Du, "Risk management study on impulse waves generated by Hongyanzi landslide in Three Gorges Reservoir of China on June 24, 2015," *Landslides*, vol. 13, no. 3, pp. 603–616, 2016.

[9] J. M. Duncan, S. G. Wright, and K. S. Wong, "Slope stability during rapid drawdown," in *Proceedings of the H. Bolton Seed Memorial Symposium*, pp. 235–272, Berkeley, CA, USA, 1990.

[10] B. Han, *Research on Landslide Monitoring and Early Warning in Ya'an Area, [Ph.D. thesis]*, China University of Geosciences, Beijing, China, 2016.

[11] F. Wang, Y. Zhang, Z. Huo, X. Peng, K. Araiba, and G. Wang, "Movement of the Shuping landslide in the first four years after the initial impoundment of the Three Gorges Dam Reservoir, China," *Landslides*, vol. 5, no. 3, pp. 321–329, 2008.

[12] W. Riemer, "Landslides and reservoirs," in *Proceedings of the 6th International Symposium on Landslide*, pp. 1373–2004, Christchurch, New ZeaLand, 1992.

[13] Committee on Reservoir Slope Stability, *Reservoir Landslides: Investigation and Management*, International Commission on Large Dams, 2002.

[14] X. Hu, M. Zhang, M. Sun, K. Huang, and Y. Song, "Deformation characteristics and failure mode of the Zhujiadian landslide in the Three Gorges Reservoir China," *Bulletin of Engineering Geology and the Environment*, vol. 74, no. 1, pp. 1–12, 2015.

[15] D. Li, K. Yin, and C. Leo, "Analysis of Baishuihe landslide influenced by the effects of reservoir water and rainfall," *Environmental Earth Sciences*, vol. 60, no. 4, pp. 677–687, 2010.

[16] M. Zhang, Y. Yin, and B. Huang, "Mechanisms of rainfall-induced landslides in gently inclined red beds in the eastern Sichuan Basin, SW China," *Landslides*, vol. 12, no. 5, pp. 973–983, 2015.

[17] M. Zhang and M. J. McSaveney, "Is air pollution causing landslides in China?," *Earth and Planetary Science Letters*, vol. 481, no. 1, pp. 284–289, 2018.

[18] M. Zhang and M. J. McSaveney, "Rock avalanche deposits store quantitative evidence on internal shear during runout," *Geophysical Research Letters*, vol. 44, no. 17, pp. 8814–8821, 2017.